JACS
JOURNAL OF THE AMERICAN CHEMICAL SOCIETY
Communication
pubs.acs.org/JACS

Achieving Site-Specificity in Multistep Colloidal Synthesis

Yuhua Feng,[†,‡] Yawen Wang,[†] Jiating He,[†] Xiaohui Song,[†] Yee Yan Tay,[§] Huey Hoon Hng,[§] Xing Yi Ling,[†] and Hongyu Chen*,[†]

[†]Division of Chemistry and Biological Chemistry, Nanyang Technological University, Singapore 637371
[‡]Department of Chemistry, Tonghua Normal University, Tonghua 134002, P.R. China
[§]School of Materials Science and Engineering, Nanyang Technological University, Singapore 639798

Supporting Information

ABSTRACT: We show that partial inhibition of the emerging Ag domain can be achieved by controlling the growth dynamics. With the symmetry broken by the "fresh" surface, sequentially growth gives (Au sphere)−(Ag wire)−(Ag plate) triblock nanostructures. This new understanding opens doors to sophisticated synthetic designs, broadening the horizon of our search for functional architectures.

Nanosynthesis is an emerging field studying the creation of nanostructures.[1] Despite tremendous progress, the synthetic capabilities are still largely limited to simple component and symmetrical nanocrystals.[2] Going beyond individual shapes, additional growth of a shaped domain onto an existing structure would enable arbitrary structural manipulation toward tailored nanohybrids.

Breaking the symmetry of colloidal nanocrystals is the central task in the pursuit of complex nanohybrids.[3] With nanoparticles freely suspended in a solution, the precise control of their growth sites is a first step toward programmable colloidal synthesis. The question is, with the same type of ligands on the same type of material surface, what are the mechanisms that can limit the directions of growth? Isotropic growth always leads to a sphere, but the crystal facets can provide a certain degree of discrimination, giving nonspherical shapes.[2a,c,4] Considering the symmetry of a crystal lattice, however, equivalent growth at the equivalent facets would lead to symmetrical crystals. For anisotropic nanocrystals, micellar templates[5] and defects[6] have been proposed to be responsible for limiting the directions of growth, giving nanowires and nanoplates. In colloidal systems, the record of restricted growth is the nanowires with only two growth directions. Hence, there is an intriguing challenge: Can we further reduce the direction of growth, so that defined shapes can emerge in only one direction?

Controlling interfacial energy is an alternative means to restrict the site of growth. Previously, ligands containing diametric −SH and −COOH groups, such as 2-mercapto-benzoimidazole-5-carboxylic acid (MBIA, Figure 1), were used to control the Ag deposition on Au seeds.[7] It can induce defects at the Au−Ag interface, shifting the overcoating growth mode (the FM mode)[8] to the island growth mode (the S−K or VW mode,[7,9] Figure 1). Basically, the Au−Ag interface increases with the expansion of the new Ag domain, but the formation of the interface is restricted by the unfavorable interfacial energy.[1]

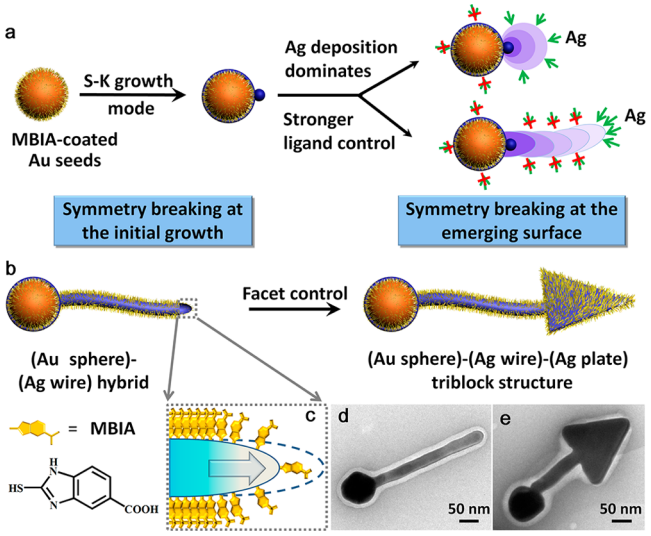

Figure 1. Schematics illustrating: (a) the difference of the symmetry breaking during the initiation of the Ag domain and the subsequent growth; (b, c) the synthesis of triblock structure with additional facet control; (d) (Au sphere)−(Ag wire) hybrid; and (e) (Au sphere)−(Ag wire)−(Ag plate) triblock nanostructure.

As a result, the symmetry is broken for the initiation of the Ag domain.

Despite the control of the Au−Ag interface, the Ag−solvent interface is newly formed with few ligands (i.e., "fresh"), leading to equivalent growth in all directions and eventually a near-spherical domain. The lack of site-specificity on this new domain makes further structural design difficult. In this work, we restrict the fresh Ag surface during the growth to break its symmetry. The dynamic but partial inhibition of the emerging Ag surface is achieved by using higher ligand concentration and slower rate of Ag reduction. With the relatively "old" surface growing older and the "fresh" surface fresher (Figure 1), the growth can be maintained at a single site, opening doors to complex growth designs.

In a typical synthesis, citrate-stabilized Au nanoparticles were used as seeds. They were incubated with ligand MBIA at 60 °C for 2 h to achieve nearly complete ligand coverage on their surface. After cooling, the reductant hydroquinone (HQ) was

Received: April 25, 2015
Published: June 9, 2015

DOI: 10.1021/jacs.5b04310
J. Am. Chem. Soc. 2015, 137, 7624−7627

added. With gentle stirring, $AgNO_3$ solution was added through a syringe pump (same amount with variable rates, 3.75−20 μL/min). The MBIA concentration was significantly higher than that used in the previous growth of Ag islands (20 μM),[7] and the Ag reduction rate was dramatically reduced with the use of syringe pump.

Direct TEM characterization of the product confirmed the successful formation of hybrid nanowires (Figure S2), but it was difficult to survey a large number of them due to the aggregation in the dried TEM sample and the presence of residue Ag salts. To avoid the problem, the product was encapsulated in polystyrene-*block*-poly(acrylic acid) (PSPAA) shells.[2c,8] After purification, the isolated polymer-coated nanostructures were characterized. Control experiments established that the encapsulation process did not affect the morphology of the Au−Ag nanohybrids. It is merely a method of preservation.

Figure 2 shows the TEM images of the Au−Ag hybrids prepared under different rates of $AgNO_3$ addition. All

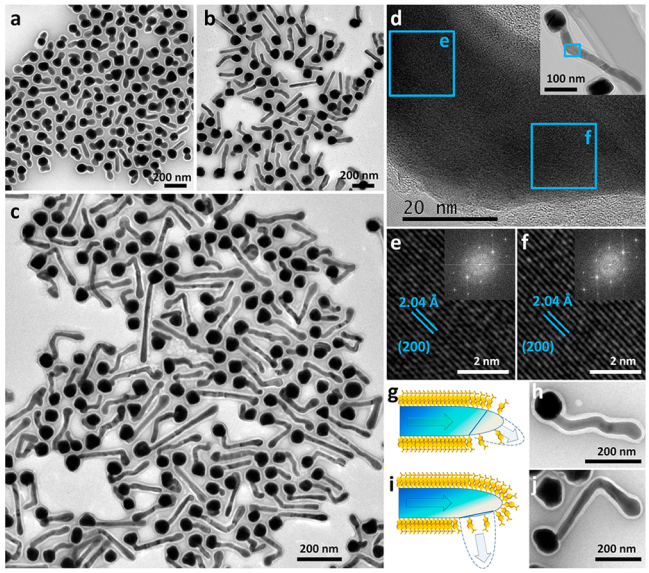

Figure 2. (Au sphere)−(Ag wire) hybrids prepared with the $AgNO_3$ injection rate of: (a) 20, (b) 5, and (c) 3.75 μL/min. (d) HRTEM image of a typical bent section; the overview is shown in the inset. (e, f) lattice fringes and FFT patterns of the highlighted areas in d. (g−j) Schematics and TEM images illustrating the shifting of growth directions.

nanostructures were coated with uniform shells of PSPAA which appeared white against the negatively stained background. When $AgNO_3$ was added at a fast rate (20 μL/min), spherical and slightly elongated Ag domains were obtained (Figure 2a). With slower rates (5 and 3.75 μL/min, all other conditions were kept the same), Ag nanowire growth was observed (Figure 2b,c), suggesting increased ligand control. The intermediates before the formation of Figure 2c were trapped. With increasing time, the Ag nanowires had roughly the same width but increasing length (Figure S3−5), suggesting continuous growth at their far end (relative to the seed).

The growth was highly specific: There was no seed with more than one nanowire attached; and no nanowire that was tethered to two seeds. It is important to note that the probability of nanowire formation decreased at the minimal rate of $AgNO_3$ addition (3.75 μL/min, Figure 2c). Only 82% of the seeds gave nanowires, in contrast to the nearly 100% probability at the higher rates of addition (Figure 2a,b). Moreover, the length distribution of the Ag nanowires also became wider (Figure S6−8), though their width was still uniform. A large percentage of the nanowires were bent with abrupt curvatures, a first indication that the growth mode is distinctively different from the micelle-templated,[5] defect-induced,[6b,c] or facet-controlled nanowire growth[9a] in the literature. We used precaution to avoid sheer-induced bending, which was ruled out as a cause by control experiments where Ag nanowires of equal width were similarly treated. Considering the rigid nanowires, the bending should more likely occur during the Ag growth.

HRTEM study of the nanowires revealed that they contained large single-crystalline domains. Figure 2d shows a typical bent section (see Figure S9), where the two selected areas across the junction are given in Figure 2e,f. The 2.04 Å *d* spacing is assigned to that of the (200) planes.[10] The alignment of these lattice fringes and of the FFT patterns suggests that the bent section is single crystalline (see Figure S9). The fact that the nanowires are wavy, along with the observation of only one set of diffraction patterns (Figure S10), can rule out five-fold twinning, which is a common structure for Ag nanowires.[11] Should the bending occur after the formation of the nanowires, the inner surface of the bend would be compressed, whereas the outer surface would be stretched. Such geometric requirements would force atomic reorganization across the bend junction, leading to multiple defects (the nanowires are thick enough that minor changes of the atomic distances would be insufficient).[12] On this basis, we believe that the bending should occur during the growth stage, where the random fluctuation of the "fresh" surface may lead to shifting of the growth directions (Figure 2g−j).

Energy dispersive X-ray spectroscopy (EDS) mapping of the (Au sphere)−(Ag nanowire) diblock nanostructures were carried out (Figure S11). The results showed that the Au seeds were covered with a thin layer of Ag, consistent with the S−K growth mode.[7,9] The nanowire section was entirely made of Ag (as opposed to Au−Ag alloy), which is expected because the Au seeds were not etched during the synthesis.

What caused the formation of a nanowire instead of an island domain? As illustrated in Figure 1, the expansion of the Ag-solvent interface is nonuniform in the former but uniform in the latter case. To resolve the mechanism, we need to understand the shift from the semi-isotropic growth to the new growth mode with symmetry breaking at the emerging Ag surface. We postulate that the slower rate of Ag deposition was indirectly responsible for the partial inhibition of the Ag surface. More specifically, the ligand coverage on a freshly generated Ag domain depends on how fast new Ag atoms are being added to the domain and how fast the ligand molecules are covering its surface. It is hard to deposit Ag once the strong ligands form a patch. Thus, the dynamic competition drives Ag atoms to the site that is relatively ligand deficient, giving a new surface layer that is even "fresher". With fewer Ag atoms being added, the ligands on the old surface gradually pack better (turn older),[1] further inhibiting growth thereon. With the right condition, only a small portion of the island/nanowire surface was able to remain fresh, while all other surfaces were inhibited. In other words, the unique nanowire growth arises because the "old" surface turns older and the "fresh" surface becomes fresher. This approach is in contrast to the previously reported substrate-bound nanowires, where the steric effect of a bulk

DOI: 10.1021/jacs.5b04310
J. Am. Chem. Soc. 2015, 137, 7624−7627

substrate was essential in maintaining a fresh surface at the seed−substrate interface.[13]

Thus, the relative location of the fresh surface at the tip of the emerging nanowire defines the direction of growth: Outward growth in the same direction gives straight nanowires (Figure 1c); slight fluctuation of the fresh surface gives wavy nanowires (Figure 2g,h); and shifting the fresh surface to the side leads to a bend (Figure 2i,j).

Such a mechanism is well consistent with our experimental observations. As the rate of $AgNO_3$ addition is reduced, so are the rates of the chemical reduction and Ag atom formation. The limited feeding of Ag atoms allows more ligands to bind to the emerging Ag domain, exacerbating the competitive growth thereon and giving nanowires. Similar competition exists among the different seeds in the solution. With limited Ag atoms, some nanoparticles were able to maintain a fresh surface, whereas others remain inhibited once they lose the competition at the initial stage (those without nanowires in Figure 2c). In contrast, with overwhelming Ag deposition, all seeds give fresh Ag islands at the initial stage, and thus, their equivalent growth leads to the near 100% nanowire formation (Figure 2b).

Interestingly, when excess amount of sodium citrate (final 1.16 mM) was added at t = 30 min after the syringe pump started, a faceted Ag nanoplate was formed at the end of each nanowire (Figure 3c). Considering the equivalent growth

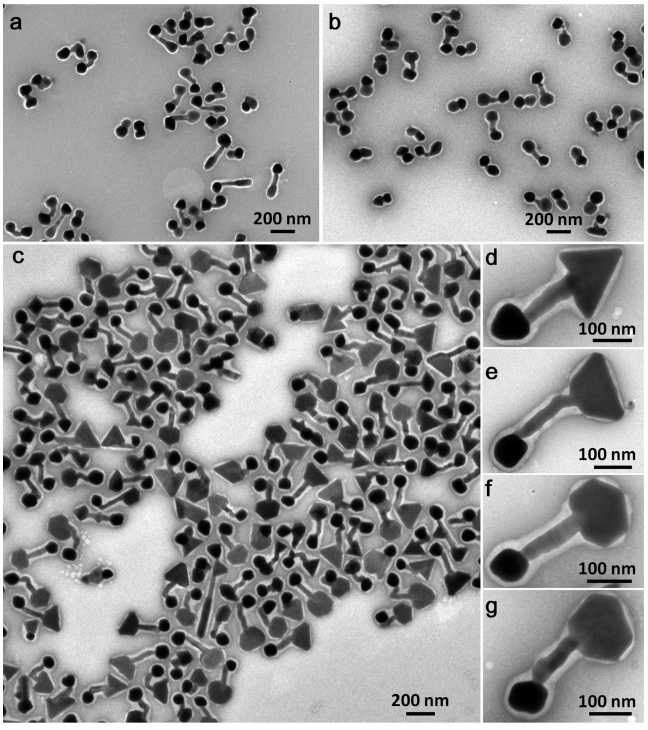

Figure 3. Trios prepared by adding (a) 0.12, (b) 0.30, and (c) 1.16 mM of sodium citrate at t = 30 min ($AgNO_3$ was injected at 5 μL/min, total lasted for 40 min). (d−g) Enlarged TEM images of the typical structures in c.

needed for the symmetry of the triangular and hexagonal prisms (as opposed to the formation of nanobelts), it appeared that the addition of citrate invalidated the control of the fresh surface. When less sodium citrate was used (0.12 and 0.3 mM), the facet formation was not obvious, but a nearly spherical domain was obtained at the far end of the nanowire (relative to the seed, Figure 3a,b). Being both ligand and reductant, the additional citrate probably promoted the reduction of $AgNO_3$, diminishing the difference between the "fresh" and "old" surfaces and causing the isotropic growth. With the increase of citrate concentration, the ligand role of citrate was obvious as Ag(111) became the most favored facet.

The plate domains are highly crystalline as evidenced by their regular shape and HRTEM. Observed along the [112] zone axis, the (−1−11), 1/2(1−31), and (2−20) diffraction spots in SAED (Figure 4b) are consistent with the Ag nanoplate with

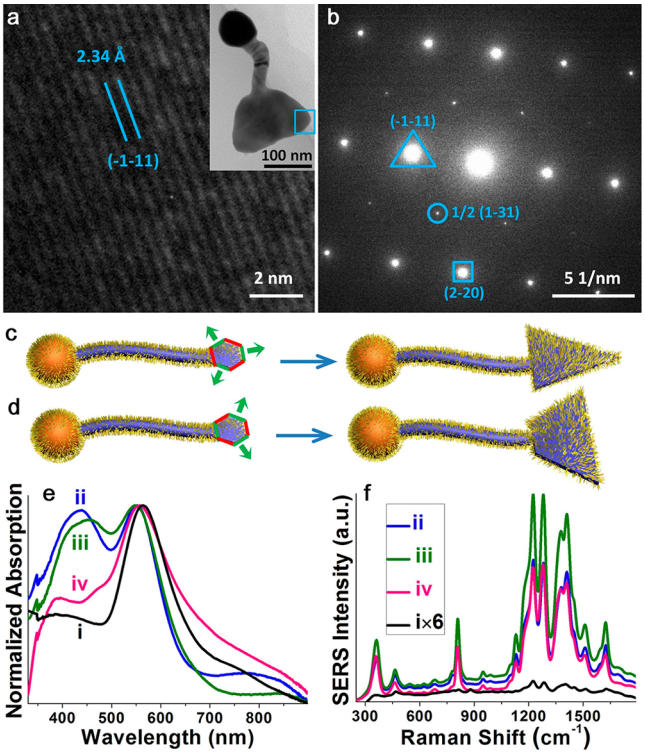

Figure 4. (a, b) HRTEM and SAED pattern (along the [112] zone axis) of the selected area, as highlighted in the inset of a. (c, d) Schematics illustrating the formation of triangular plates. (e) Extinction and (f) SERS spectra of (i) the MBIA-functionalized Au seeds and (ii−iv) the triblock structures as shown in (ii) Figure 3a; (iii) 3b and (iv) 3c.

the top and bottom surfaces being Ag(111) facets.[14] In particular, the appearance of the forbidden 1/2(131) spots (corresponding to a 2.50 Å lattice spacing) indicates that the lattice is not a perfect fcc. These spots are equivalent to the 1/3(422) spots observed at the [111] zone axis[14a] (by tilting the [112] diffraction pattern 19°), which were frequently observed in Au and Ag nanoplates.[6e,14a,15] As proposed previously, these forbidden spots are indicative of a horizontal twin plane along the Ag plate.[14,16] From the point of crystal growth mechanism, the twin plane is believed to be responsible for the symmetry breaking, i.e., only one out of the four stable Ag/Pd(111) facets was preferred when forming Ag and Pd plates.[6e,11,15a,17] More specifically, the twin defect leads to concave and convex edges in the hexagonal nucleus, and the preferential growth at the concave edges (the reentrant grooves) eventually leads to a triangular plate.[15b,16] As shown in Figure 4c,d, the observation of forward and inverted triangular domains is well consistent with this mechanism. The concurrent hexagonal nanoplates are also consistent, as they are known to be the consequence of two parallel twin-plane defects.[15b]

DOI: 10.1021/jacs.5b04310
J. Am. Chem. Soc. 2015, 137, 7624−7627

The UV−vis spectra (Figure 4e) indicate the formation of Ag domains with the increasing absorption at 410 nm due to Ag plasmon resonance. The absorption at around 540 nm has contributions from both the Au sphere[7] and the Ag plate.[6e] Figure 4f shows the great enhancement of SERS signal as compared to the already enhanced signals of the MBIA-functionalized Au seeds (by about 50−70 times). But considering the Ag domains with different sizes and shapes, assigning the SERS contribution is difficult.

In our system, the Ag surface is only partially inhibited, whereas in the conventional mechanisms, the inhibition is highly facet specific, where one set of facets is either all inhibited or not. Moreover, due to lack of site selectivity, the typical seeded growth in the literature gave only individual nanocrystals, not as an additional domain on an existing structure. The difference between the current and conventional systems can be attributed, at least partially, to the use of strong ligands. The affinity of SH-ended MBIA on Ag surface is much stronger than the typical ligands in the literature. For weak ligands, the difference between "old" and "fresh" surfaces is expected to be less dramatic, making it difficult to exploit the "fresh" surface.

In conclusion, we report the sequential growth of shaped domains in a single direction on freely suspended colloidal nanoparticles. The resulting (Au sphere)−(Ag wire)−(Ag plate) triblock nanostructure is the first example, to the best of our knowledge, where three discrete shapes are combined via bottom-up processes. Most importantly, our demonstrated ability in the dynamic control of "fresh" and "old" surfaces allows selective growth in a single direction. Such site selectivity allows symmetry breaking of the typical nanoparticles. It is essential in building sophisticated structural features, and it may eventually lead us beyond the current nanotechnology, where most the applications are based on simple structures.

■ ASSOCIATED CONTENT

Supporting Information

Materials, methods, and large area view of TEM images. The Supporting Information is available free of charge on the ACS Publications website at DOI: 10.1021/jacs.5b04310.

■ AUTHOR INFORMATION

Corresponding Author

*hongyuchen@ntu.edu.sg

Notes

The authors declare no competing financial interest.

■ ACKNOWLEDGMENTS

This work was supported by the A*STAR of Singapore (SERC 112-120-2011), the MOE of Singapore (RG14/13), and the National Research Foundation of Singapore (NRF) (Sustainable Energy (SinBeRISE) CREATE Program through the Singapore-Berkeley Research Initiative).

■ REFERENCES

(1) Wang, Y.; He, J.; Liu, C.; Chong, W. H.; Chen, H. *Angew. Chem., Int. Ed.* **2015**, *54*, 2022.

(2) (a) Xia, Y.; Xiong, Y.; Lim, B.; Skrabalak, S. E. *Angew. Chem., Int. Ed.* **2009**, *48*, 60. (b) You, H.; Yang, S.; Ding, B.; Yang, H. *Chem. Soc. Rev.* **2013**, *42*, 2880. (c) Tao, A. R.; Habas, S.; Yang, P. *Small* **2008**, *4*, 310.

(3) (a) Xia, X.; Xia, Y. *Nano Lett.* **2012**, *12*, 6038. (b) Zeng, J.; Zhu, C.; Tao, J.; Jin, M.; Zhang, H.; Li, Z.-Y.; Zhu, Y.; Xia, Y. *Angew. Chem., Int. Ed.* **2012**, *51*, 2354.

(4) (a) Niu, W.; Zheng, S.; Wang, D.; Liu, X.; Li, H.; Han, S.; Chen, J.; Tang, Z.; Xu, G. *J. Am. Chem. Soc.* **2009**, *131*, 697. (b) Wang, X.; Zhuang, J.; Peng, Q.; Li, Y. *Nature* **2005**, *437*, 121. (c) Xiong, S.; Xi, B.; Zhang, K.; Chen, Y.; Jiang, J.; Hu, J.; Zeng, H. C. *Sci. Rep.* **2013**, *3*, 2177.

(5) (a) Huo, Z.; Tsung, C.-k.; Huang, W.; Zhang, X.; Yang, P. *Nano Lett.* **2008**, *8*, 2041. (b) Jana, N. R.; Gearheart, L.; Murphy, C. J. *Adv. Mater.* **2001**, *13*, 1389.

(6) (a) Zhu, L.; Shen, X.; Zeng, Z.; Wang, H.; Zhang, H.; Chen, H. *ACS Nano* **2012**, *6*, 6033. (b) Sun, Y.; Ren, Y.; Liu, Y.; Wen, J.; Okasinski, J. S.; Miller, D. J. *Nat. Commun.* **2012**, *3*, 971. (c) Meng, F.; Morin, S. A.; Forticaux, A.; Jin, S. *Acc. Chem. Res.* **2013**, *46*, 1616. (d) Millstone, J. E.; Hurst, S. J.; Métraux, G. S.; Cutler, J. I.; Mirkin, C. A. *Small* **2009**, *5*, 646. (e) Zhang, Q.; Li, N.; Goebl, J.; Lu, Z.; Yin, Y. *J. Am. Chem. Soc.* **2011**, *133*, 18931. (f) Jin, R.; Charles Cao, Y.; Hao, E.; Metraux, G. S.; Schatz, G. C.; Mirkin, C. A. *Nature* **2003**, *425*, 487. (g) Jin, R.; Cao, Y.; Mirkin, C. A.; Kelly, K. L.; Schatz, G. C.; Zheng, J. G. *Science* **2001**, *294*, 1901.

(7) Feng, Y.; He, J.; Wang, H.; Tay, Y. Y.; Sun, H.; Zhu, L.; Chen, H. *J. Am. Chem. Soc.* **2012**, *134*, 2004.

(8) Feng, Y.; Wang, Y.; Wang, H.; Chen, T.; Tay, Y. Y.; Yao, L.; Yan, Q.; Li, S.; Chen, H. *Small* **2012**, *8*, 246.

(9) (a) Bauer, E. *Z. Kristallogr.* **1958**, *110*, 372. (b) Peng, Z.; Yang, H. *Nano Today* **2009**, *4*, 143.

(10) Zhang, D.; Qi, L.; Ma, J.; Cheng, H. *Chem. Mater.* **2001**, *13*, 2753.

(11) Elechiguerra, J. L.; Reyes-Gasga, J.; Yacaman, M. J. *J. Mater. Chem.* **2006**, *16*, 3906.

(12) Xu, J.; Wang, Y.; Qi, X.; Liu, C.; He, J.; Zhang, H.; Chen, H. *Angew. Chem., Int. Ed.* **2013**, *52*, 6019.

(13) He, J.; Wang, Y.; Feng, Y.; Qi, X.; Zeng, Z.; Liu, Q.; Teo, W. S.; Gan, C. L.; Zhang, H.; Chen, H. *ACS Nano* **2013**, *7*, 2733.

(14) (a) Reyes-Gasga, J.; Gómez-Rodríguez, A.; Gao, X.; José-Yacamán, M. *Ultramicroscopy* **2008**, *108*, 929. (b) Mendoza-Resendez, R.; Nunez, N. O.; Barriga-Castro, E. D.; Luna, C. *RSC Adv.* **2013**, *3*, 20765.

(15) (a) Germain, V.; Li, J.; Ingert, D.; Wang, Z. L.; Pileni, M. P. *J. Phys. Chem. B* **2003**, *107*, 8717. (b) Lofton, C.; Sigmund, W. *Adv. Funct. Mater.* **2005**, *15*, 1197. (c) Millstone, J. E.; Métraux, G. S.; Mirkin, C. A. *Adv. Funct. Mater.* **2006**, *16*, 1209.

(16) Kirkland, A. I.; Jefferson, D. A.; Duff, D. G.; Edwards, P. P.; Gameson, I.; Johnson, B. F. G.; Smith, D. J. *Proc. R. Soc. London, Ser. A* **1993**, *440*, 589.

(17) Huang, X.; Tang, S.; Mu, X.; Dai, Y.; Chen, G.; Zhou, Z.; Ruan, F.; Yang, Z.; Zheng, N. *Nat. Nano* **2011**, *6*, 28.

DOI: 10.1021/jacs.5b04310
J. Am. Chem. Soc. 2015, 137, 7624−7627